

Introduction

Planet formation starts with coagulation of μm dust and ice grains; in a later stage Planets are formed by accretion of km-sized objects, the planetesimals. The processes involved in the growth of the planetesimals are not yet understood entirely, as different mechanisms, e.g. bouncing and fragmentation, can prevent further growth. Two main groups of models try to explain planetesimal growth: coagulation in mutual collisions and gravitational instabilities in areas of high particle concentration. The collision dynamics of dm bodies are important for coagulation models, as dm bodies start to decouple from the surrounding gas and drift towards the star. They are also important for gravitational instability models, as dm bodies are believed to be affected the strongest by particle concentration mechanisms, e.g. streaming instability. We investigated collisions of cm onto dm dust agglomerates at around 7 ms^{-1} , which can very well represent the collisions of such bodies at 1 AU in protoplanetary discs. In addition to that we show first results of collisions with solid dm ice, as beyond the snow line water ice is dominant and the formation of icy planetesimals possible.

Experiment

Setup for the Ice Collisions

- collisions of **solid ice** in a deep freezer ($T \approx -17 \text{ }^\circ\text{C}$)
- projectiles accelerated towards the target by a **crossbow**
- collisions observed by a high speed camera at **5000 fps**

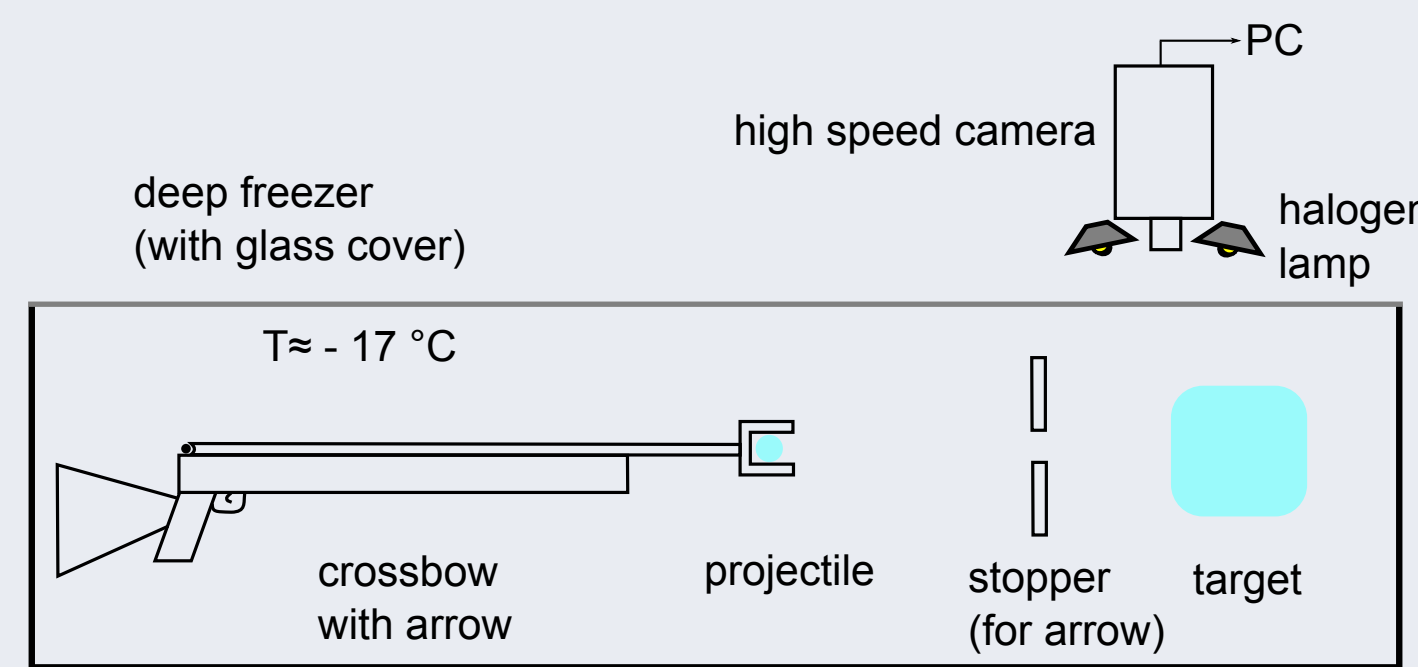


Figure 1: Experimental Setup for the Ice Collisions

Setup for the Dust Collisions

- Experiments in a small drop tower (3m high) under vacuum conditions ($p \leq 1.5 \times 10^{-1} \text{ mbar}$)
- projectiles ($m = 2.5 - 20 \text{ g}$, $d = 1.5 - 3 \text{ cm}$) and targets ($m \approx 1.5 \text{ kg}$, $d = h = 12 \text{ cm}$) are made up of quartz powder with μm grains
- mean volume filling factors of 0.44 (targets) and 0.466 (projectiles)
- collisions observed by a high speed camera (500 fps) and illuminated by halogen lamps



Figure 2: Press with dust agglomerate

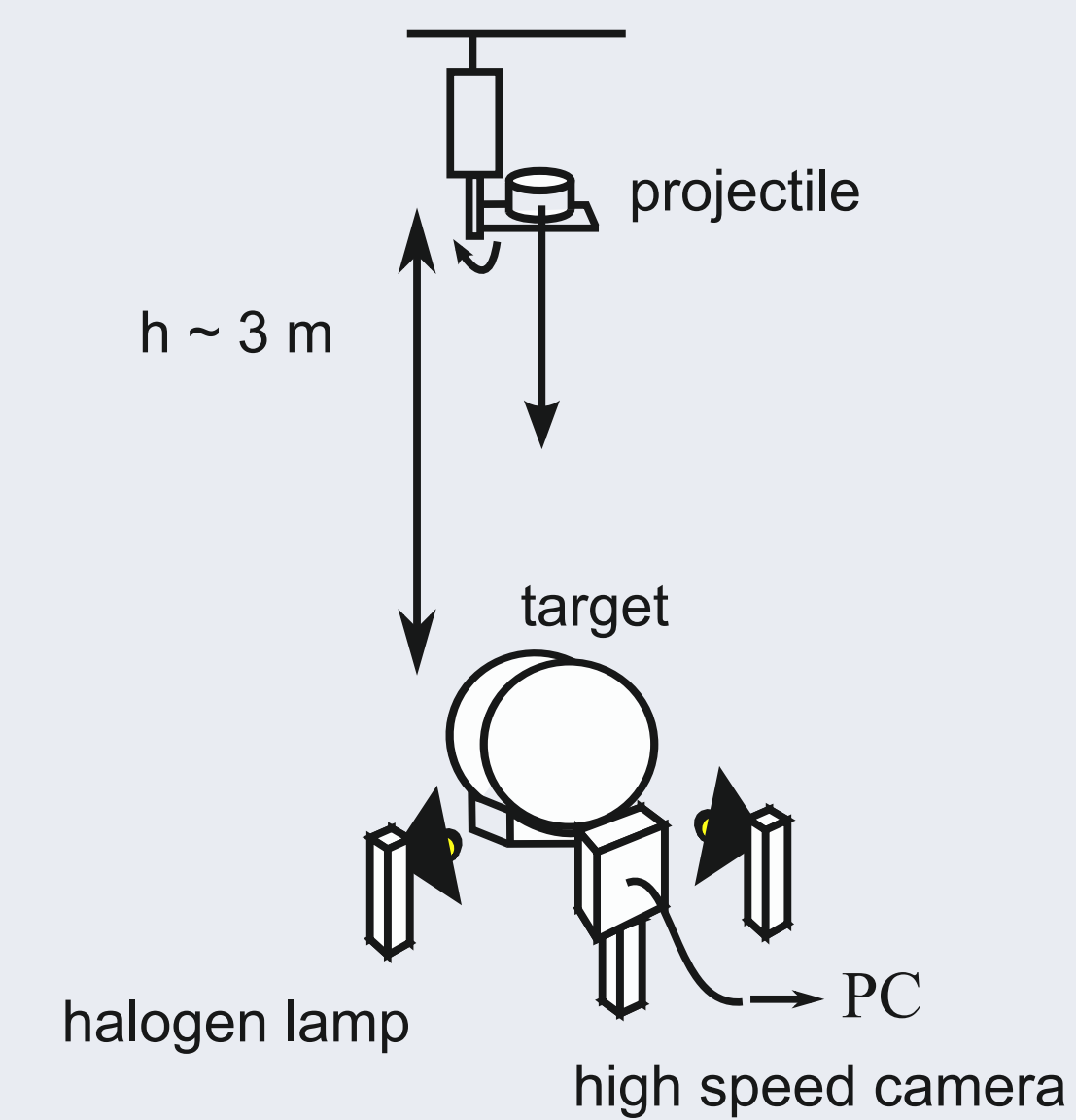


Figure 3: Setup for the Dust Collisions

Results and Discussion

First Results of the Ice Collisions

- collisions of projectiles of different diameters (1.7 - 3.3 cm) and targets with $d = h = 12 \text{ cm}$ at velocities of 20 - 43 m s^{-1}
- projectiles have masses of 2 - 17 g, target: $m \approx 1.2 \text{ kg}$
- two outcomes are observed: collisions with and without **mass transfer** from projectile to target
- in both cases the projectiles get disrupted and cause slight damage to the target surface (small crack)
- transition velocity between the two cases decreases with increasing projectile size (dashed lines in Fig. 4)
- no mass gain in collisions with projectiles of $d = 3.3 \text{ cm}$
- only a small amount of the projectile is transferred, the accretion efficiency is less than 2%

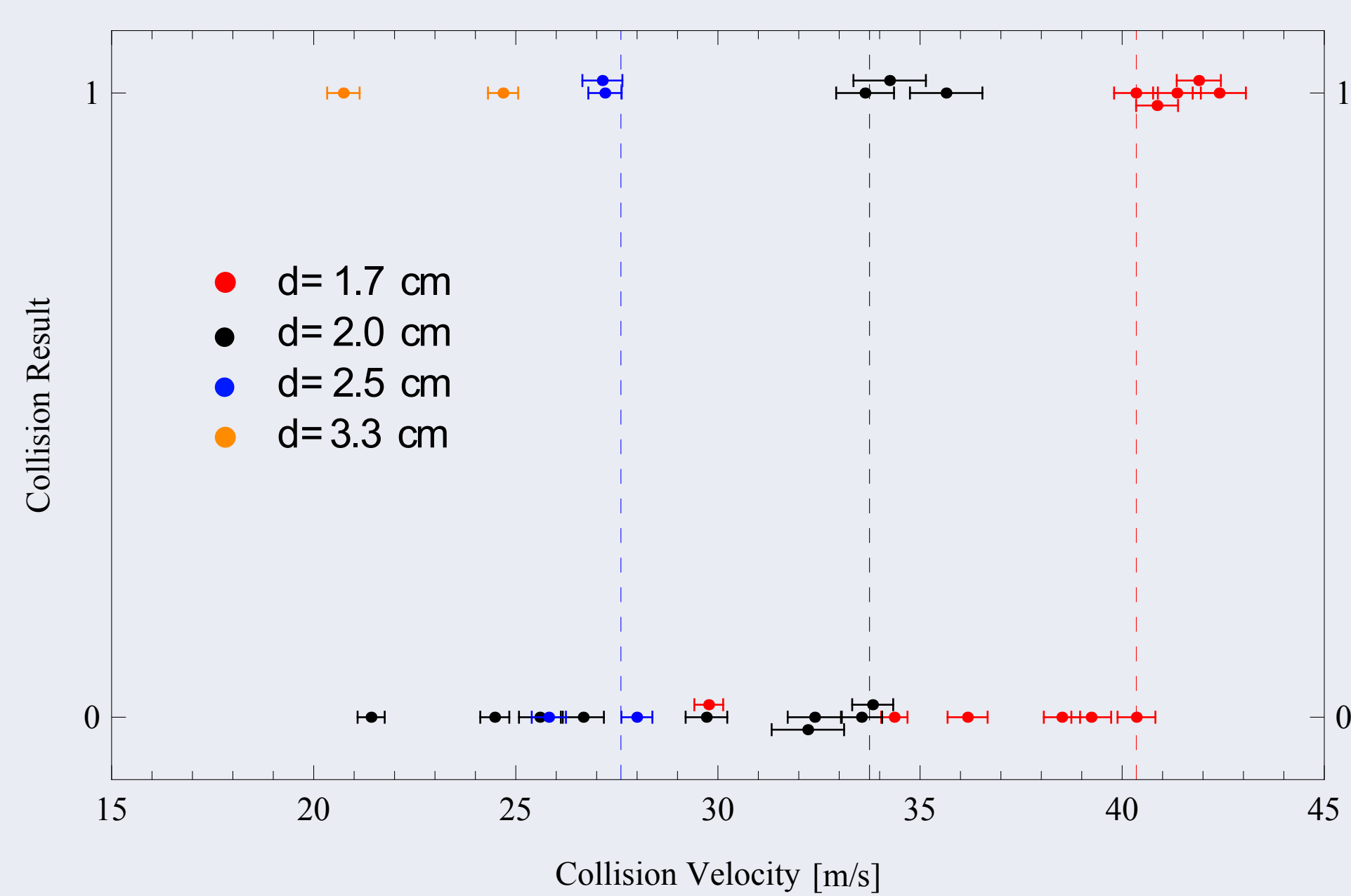


Figure 5: Results of the collisions (0 = mass gain, 1 = no mass gain) for collisions with projectiles of different diameters (data points are moved slightly on the y-axis for better visibility)

Results of the Dust Collisions

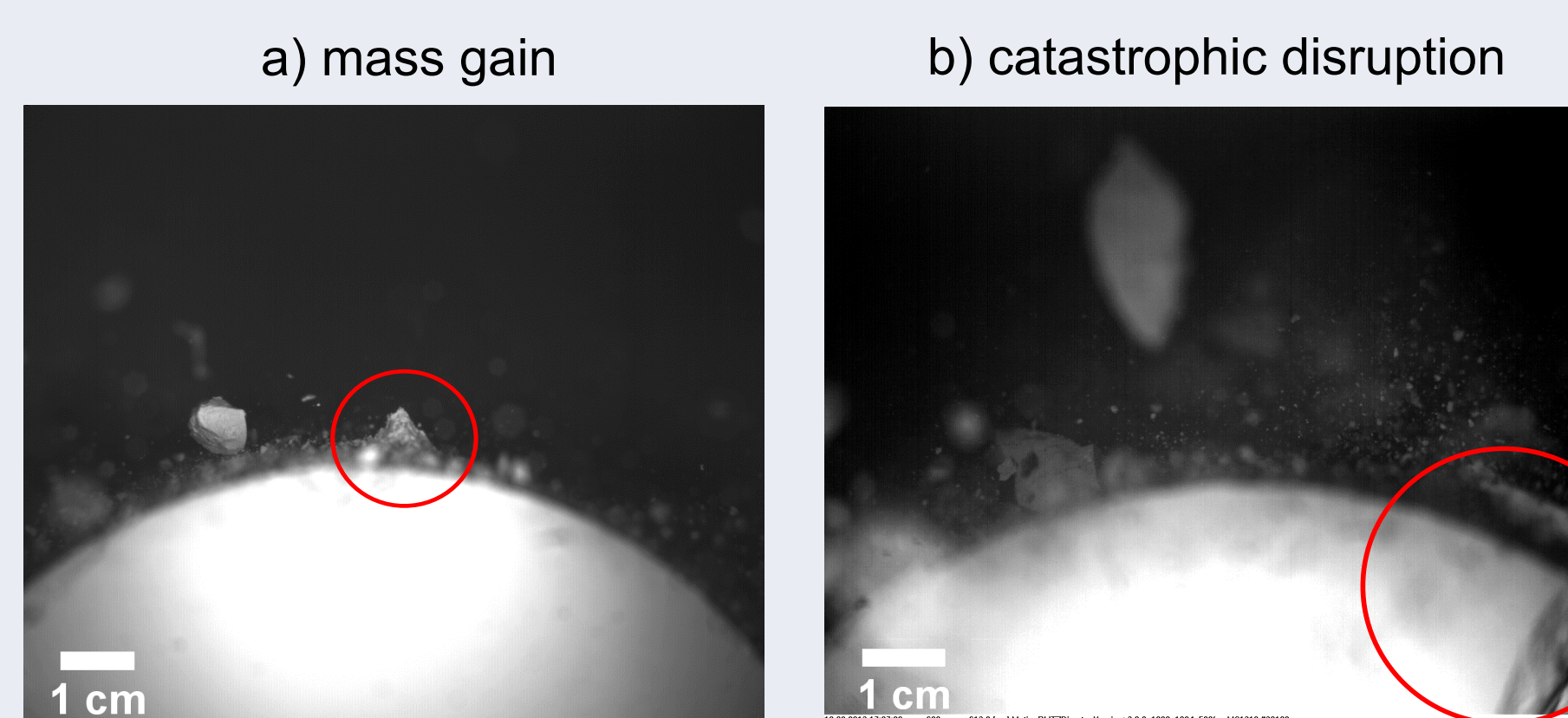


Figure 4: Example for a collision with mass gain and one with catastrophic disruption (Deckers and Teiser 2014)

- mean collision velocity of $6.68 \pm 0.67 \text{ m s}^{-1}$
- two different outcomes of collisions are observed (see red circles in Fig. 4)
- direct transition between mass gain and catastrophic disruption of the target
- fracture lines are independent of the collision point and lie perpendicular to the symmetry axis

Fragmentation Strength

- linear and rotational movement are derived from the camera images
- kinetic energy of a projectile is defined as: $E_{\text{kin}} = 1/2 (mv^2 + I_x \omega_x^2 + I_y \omega_y^2)$
- the mass balance, i.e. sticking mass or largest target fragment, is determined with a scale
- the threshold is at $298 \pm 25 \text{ mJ}$, which corresponds to a **fragmentation strength** of $Q^* = 190 \pm 16 \text{ mJ kg}^{-1}$

Accretion Efficiency e_{ac}

- depend on collision parameters: kinetic energy, impact angle α , difference in filling factor ($\Delta\Phi = \Phi_p - \Phi_t$)
- analytical formula describing the dependencies: $e_{\text{ac}}(E_{\text{kin}}, \Delta\Phi, \alpha) = e_{\text{ac},0} + 0.025\%/m\text{J } E_{\text{kin}} - 49\%\Delta\Phi - c_r/\alpha$
- can easily be included into coagulation models (e.g. Drazkowska et al. 2013)

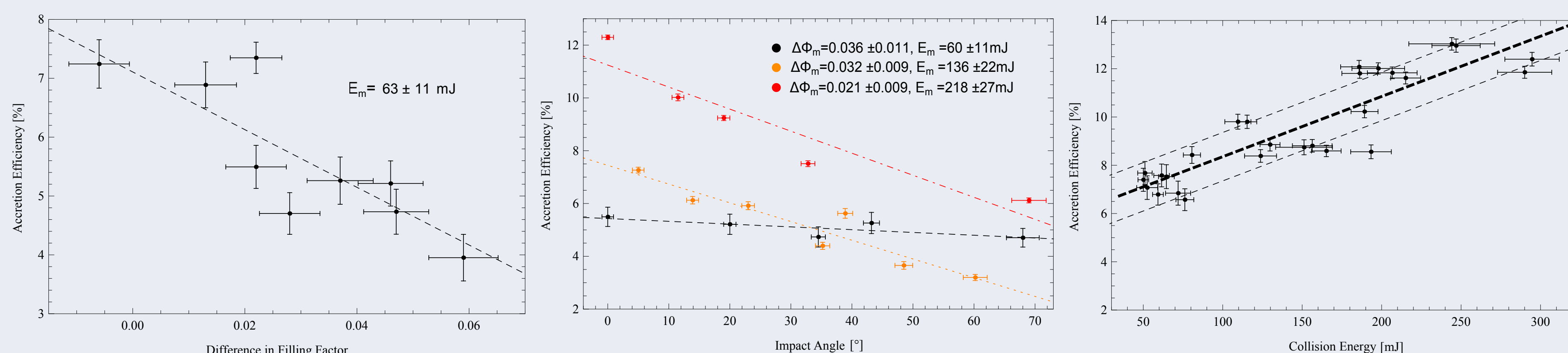


Figure 6: Dependency of the accretion efficiency on different collision parameters (Deckers and Teiser 2014)

Conclusions

- mass gain of the dm body at velocities of up to 40 ms^{-1}
- transition velocity decreases with increasing projectile size

- the fragmentation strength of dm dust agglomerates is at $Q^* = 190 \text{ mJ kg}^{-1}$, a factor 4 larger than expected
- growth of the dm body through mass transfer, accretion efficiency depends on different collision parameters
- re-accretion of slow small projectile ejecta possible, which can enhance the growth further

References

- [1] A. Johansen et al., "Rapid planetesimal formation in turbulent circumstellar disks", Nature, 448, 2007.
- [2] J. Deckers and J. Teiser, "Macroscopic Dust in Protoplanetary Disks - From Growth to Destruction", ApJ (accepted).
- [3] J. Deckers and J. Teiser, "Colliding Decimeter Dust", ApJ, 769, 2013.
- [4] J. Drazkowska et al, "Planetesimal formation via sweep up growth at the inner edge of dead zones", A&A, 556, 2013
- [5] Y. Shimaki and M. Arakawa, "Experimental study on collisional disruption of highly porous icy bodies", Icarus, 218, 2012.

Acknowledgements

We thank the Deutsche Forschungsgemeinschaft (DFG) for their funding within the frame of the SPP 1385.